BMB Reports - Manuscript Submission

Manuscript Draft

Manuscript Number: BMB-18-231

Title: Protective effects of N,4,5-trimethylthiazol-2-amine hydrochloride on hypoxia-induced β-amyloid production in SH-SY5Y cells

Article Type: Article

Keywords: N,4,5-trimethylthiazol-2-amine hydrochloride; hypoxia; amyloid protein; ischemia

Corresponding Author: Sung-Woo Cho

Authors: A Reum Han[1], Ji Woong Yang[1], Jung-Min Na[1], Soo Young Choi[2], Sung-Woo Cho[1,*]

Institution: [1]Biochemistry and Molecular Biology, University of Ulsan College of Medicine,
[2]Biomedical Science and Research Institute of Bioscience and Biotechnology, Hallym University,

Protective effects of *N*,4,5-trimethylthiazol-2-amine hydrochloride on hypoxia-induced β-amyloid production in SH-SY5Y cells

A Reum Han[a], Ji Woong Yang[a], Jung-Min Na[a], Soo Young Choi[b], and Sung-Woo Cho[a,*]

[a]*Department of Biochemistry and Molecular Biology, University of Ulsan College of Medicine, Seoul 05505, Korea*

[b]*Department of Biomedical Science and Research Institute of Bioscience and Biotechnology, Hallym University, Gangwon 24252, Korea*

Running title: KHG21702 protects hypoxia-induced Aβ production

*Corresponding author.
E-mail address: swcho@amc.seoul.kr (S.-W. Cho)

ABSTRACT

Although hypoxic/ischemic injury is thought to contribute to the incidence of Alzheimer's disease (AD), the molecular mechanism that determines the relationship between hypoxia-induced β-amyloid (Aβ) generation and development of AD is not yet known. We have now investigated the protective effects of *N*,4,5-trimethylthiazol-2-amine hydrochloride (KHG26702), a novel thiazole derivative, on oxygen–glucose deprivation (OGD)–reoxygenation (OGD–R)-induced Aβ production in SH-SY5Y human neuroblastoma cells. Pretreatment of these cells with KHG26702 significantly attenuated OGD–R-induced production of reactive oxygen species and elevation of levels of malondialdehyde, prostaglandin E_2, interleukin 6 and glutathione, as well as superoxide dismutase activity. KHG26702 also reduced OGD–R-induced expression of the apoptotic protein caspase-3, the apoptosis regulator Bcl-2, and the autophagy protein becn-1. Finally, KHG26702 reduced OGD–R-induced Aβ production and cleavage of amyloid precursor protein, by inhibiting secretase activity and suppressing the autophagic pathway. Although supporting data from *in vivo* studies are required, our results indicate that KHG26702 may prevent neuronal cell damage from OGD–R-induced toxicity.

Keywords: N,4,5-trimethylthiazol-2-amine hydrochloride; hypoxia; amyloid protein; ischemia

INTRODUCTION

Ischemia–reperfusion results in neuronal cell damage, and ischemia–reperfusion-induced oxidative stress is closely related to the pathogenesis of cerebral ischemia (1). Hypoxic/ischemic injury contributes to the incidence of Alzheimer's disease (AD), which is the most common type of dementia (2-5). One of the major risk factors for AD is accumulation of β-amyloid (Aβ) that is produced in the brain from amyloid precursor protein (APP) by APP-cleaving enzymes, including β-secretase and γ-secretase (6). Notably, hypoxia induces abnormal processing of APP by activating these secretases (6, 7). However, the molecular mechanism underlying the relationship between hypoxia-induced Aβ generation and development of AD pathogenesis is not yet known.

The nervous system is especially vulnerable to hypoxic injury because of its high consumption of oxygen and low capacity for regeneration (8, 9). Effective neuroprotective strategies against irreversible hypoxic injury have not yet been developed. Accordingly, systematic searching may be necessary to discover novel pharmacological agents for the amelioration of hypoxic damage. Our strategy has been to synthesize structurally distinct compounds and to investigate their ability to control neuronal injury. Among such compounds, thiazole derivatives have been shown to have neuroprotective properties. For instance, AS601245, a benzothiazole derivative, showed protective effects in focal brain ischemia (10). In addition, a protective effect of another thiazole derivative on Aβ-induced neurotoxicity has been reported in cultured neurons (11). However, precise mechanisms for the activities of these agents have not yet been identified.

In the present study, we have, for the first time, investigated the protective effects and mechanisms of action of *N*,4,5-trimethylthiazol-2-amine hydrochloride (KHG26702), a novel thiazole derivative, in oxygen–glucose deprivation (OGD)–reoxygenation (OGD–R)-induced

Aβ production in SH-SY5Y human neuroblastoma cells.

RESULTS AND DISCUSSION

KHG26702 alleviates OGD–R-induced toxicity in SH-SY5Y cells

Complex mechanisms are responsible for neuronal cell death following ischemia. In this study, we aimed to explore the protective properties of KHG26702, a novel thiazole amine derivative (Fig. 1A), in relation to an important aspect of this process. For this purpose, we adapted cultured SH-SY5Y human neuroblastoma cells under OGD–R conditions as a model of ischemia–reperfusion injury, in the knowledge that exposure of differentiated SH-SY5Y cells to OGD leads to ischemia-induced cell death (12, 13). We first investigated the effect of KHG26702 on cell viability and lactate dehydrogenase (LDH) release from SH-SY5Y cells exposed to OGD–R. Viability of SH-SY5Y cells after 5 h OGD followed by 20 h reoxygenation was reduced to 35% of that in untreated control cells (Fig. 1B). Pretreatment with KHG26702 dose-dependently protected the cells from OGD–R-induced toxicity, and with 5 μM KHG26702, cell viability was almost at the level of the control cells (Fig. 1B). In the absence of OGD–R, KHG26702 itself had no effect on cell viability (Fig. 1B).

The effect of KHG26702 on OGD–R-induced cell death was further examined by measuring LDH activity, which is an indicator of cellular damage. Exposure of SH-SY5Y cells to OGD–R increased LDH activity up to 1.8-fold compared with the activity in control cells (Fig. 1C). Notably, pretreatment of SH-SY5Y cells with 5 μM KHG26702 significantly reduced OGD–R-induced LDH leakage (Fig. 1C). In these experiments, KHG26702 effectively prevented OGD–R-induced toxicity in SH-SY5Y cells. The concentration of KHG26702 was fixed at 5 μM for all subsequent experiments.

Effects of OGD–R and KHG26702 on markers of oxidative stress, inflammation, and antioxidant activity in SH-SY5Y cells

Upregulation of levels of reactive oxygen species (ROS) in the brains of experimental animal models of hypoxia leads to cell death (12-14), and ROS-induced oxidative damage may be an important factor in ischemia–reperfusion-induced neuronal cell death (14). Antioxidants that reduce ROS production in hypoxic conditions may therefore have neuroprotective potential, so we measured the effects of KHG26702 on OGD–R-induced ROS levels. In OGD–R-induced cells, ROS levels were almost twice as high as in control cells (Fig. 2A). Pretreatment with KHG26702 significantly reduced ROS induction (Fig. 2A), suggesting that it had an antioxidant role.

A rapid increase in lipid peroxidation during global ischemia may be a factor that contributes to neuronal cell death (15). We found that OGD–R-exposed cells had higher levels of malondialdehyde (MDA) than control cells (Fig. 2B). KHG26702 pretreatment efficiently suppressed the increase in MDA (Fig. 2B). These results demonstrated that KHG26702 could attenuate OGD–R-induced oxidative stress by reducing ROS generation and lipid peroxidation.

We investigated the effects of KHG26702 on the OGD–R-induced production of inflammatory factors by measuring levels of prostaglandin E_2 (PGE_2) and interleukin 6 (IL-6) in conditioned culture media by enzyme-linked immunosorbent assay (ELISA). OGD–R induced upregulation of these factors, which was particularly strong for PGE_2 (Fig. 2C). KHG26702 pretreatment significantly reduced upregulation of PGE_2, and completely prevented upregulation of IL-6 (Fig. 2C, D), suggesting that the mechanisms underlying the effects of KHG26702 on OGD–R-induced cell death may involve the regulation of mediators of inflammation. The lack of toxicity of KHG26702 in SH-SY5Y cells (Fig. 1) indicates that

its anti-inflammatory effects were not the result of drug-induced cell death. These findings suggest that KHG26702 has therapeutic potential for the management of neuroinflammatory diseases.

Antioxidant enzymes such as superoxide dismutase (SOD) constitute a central defense system against ROS production, because they can degrade ROS directly (16). Furthermore, SOD protects brain tissues by eliminating free radicals resulting from ischemic injury (17). Reduced glutathione (GSH) also has important roles in cellular defenses against ROS (18). Therefore, induction of antioxidants may help to overcome oxidative-stress-related neuropathology. Here, we found that SOD activity and GSH levels were substantially reduced by OGD–R, but pretreatment with KHG26702 largely prevented these reductions (Fig. 2E, F), indicating its antioxidant potential.

Effects of OGD–R and KHG26702 on expression of the apoptosis-related proteins caspase-3 and Bcl-2

Activation of caspase-3 can be detected in ischemic brain tissue, causing hypoxia/ischemia-induced apoptotic neuronal cell death (19, 20, 21). By contrast, Bcl-2 is an important anti-apoptotic protein, which improves cellular survival by suppressing the actions of pro-apoptotic proteins. Overexpression of Bcl-2 can reduce caspase-3 activity and ischemic neuronal damage in an experimental model of stroke (22).

By western blotting, we found that OGD–R reduced levels of Bcl-2 and increased levels of activated caspase-3 in SH-SY5Y cells, compared with untreated controls (Fig. 3A–C). However, pretreatment with KHG26702 significantly reduced the effect of OGD–R on caspase-3, and prevented any reduction in Bcl-2 (Fig. 3A–C), demonstrating the potential of KHG26702 to protect against OGD–R-induced apoptosis by regulating Bcl-2 and caspase-3.

Effects of OGD–R and KHG26702 on Aβ levels, secretase activity, and becn-1 levels

The accumulation of Aβ to form senile plaques is a characteristic feature of AD, and Aβ has a crucial role in the development of neuronal damage leading to cognitive deficits in learning and memory (24, 25). Aβ is associated with impairment of synaptic function and with the risk of developing AD (26, 27). Hypoxia/ischemia can activate expression of APP in the brain, contributing to the development of AD (2, 4). Aβ is produced by cleavage of APP by β-secretase and γ-secretase (28, 29), and elevation of expression and activities of these secretases occurs in neuronal cells and brain tissue under hypoxic/ischemic conditions, leading to Aβ production and accumulation of amyloid plaques (3, 5).

Here, we used ELISA to investigate the effects of OGD–R and KHG26702 on Aβ production in SH-SY5Y cells. Levels of secreted $A\beta_{40}$ and $A\beta_{42}$ were higher with OGD–R than with no treatment, but KHG26702 pretreatment significantly attenuated this upregulation (Fig. 4A, B). Similarly, the activities of β-secretase and γ-secretase were higher in OGD–R-treated cells than in controls, and this upregulation was attenuated by pretreatment with KHG26702 (Fig. 4C, D). These results suggest that KHG26702 protects neuronal cells from the effects of hypoxia by suppression of Aβ generation via downregulation of β- and γ-secretase activities. The ability of KHG26702 to lower Aβ levels may be of clinical benefit.

Finally, we investigated the effects of KHG26702 on levels of the autophagy protein becn-1 in OGD–R-induced SH-SY5Y cells, because autophagic vacuoles contain APP and γ-secretase, and neuronal macroautophagy is activated in AD (30). Furthermore, hypoxia increases γ-secretase cleavage of APP via activation of macroautophagy in a mouse model of AD (7). By western blotting, we identified a 6.2-fold higher level of becn-1 in OGD–R-treated SH-SY5Y cells than in untreated controls (Fig. 4E, F), indicating activation of autophagic status during the hypoxic event. Notably, KHG26702 pretreatment prevented OGD–R-induced upregulation of becn-1 (Fig. 4E, F). Our results indicate that KHG26702

reduced Aβ production and cleavage of APP by inhibiting secretase activities and suppressing the autophagic pathway in OGD–R-induced SH-SY5Y cells.

Collectively, our results showed that KHG26702 can significantly reduce OGD–R-induced Aβ production in SH-SY5Y cells. KHG26702 pretreatment inhibited OGD–R-induced cell death and oxidative stress, and reduced Aβ production and cleavage of APP by inhibiting secretase activities and suppressing autophagy. However, other mechanisms by which KHG26702 may attenuate OGD–R-induced SH-SY5Y cell injury cannot yet be completely excluded. Supporting data from *in vivo* studies will be required to further our understanding of the mechanisms of action of this novel compound.

MATERIALS AND METHODS

Materials

Phosphate-buffered saline, dimethyl sulfoxide, Dulbecco modified Eagle's medium, fetal calf serum, L-glutamine, penicillin, and streptomycin were obtained from Sigma-Aldrich (St Louis, MO, USA). Antibodies against caspase-3, Bcl-2, becn-1, and β-actin were purchased from Cell Signaling Technology (Beverly, MA, USA). All other reagents were of the highest purity among commercially available products.

Synthesis of *N*,4,5-trimethylthiazol-2-amine hydrochloride (KHG26702)

To a solution of 0.2 g (2.2 mmol) 1-methyl thiourea dissolved in 3 mL of ethanol was added 0.24 mL (2.2 mmol) of 3-chloro-2-butanone, and the reaction mixture was refluxed for 8 h. The solvent was removed by evaporation to leave a solid product, which was dissolved in methylene chloride, washed with water, and then dried with anhydrous $MgSO_4$. After filtration, the filtrate was evaporated to give *N*,4,5-trimethylthiazol-2-amine hydrochloride (0.401 g, 68%) as a white solid.

Cell culture and OGD–R

SH-SY5Y cells were cultured in Dulbecco modified Eagle's medium supplemented with 5% fetal calf serum, 100 mg/mL streptomycin, 100 U/mL penicillin, and 2 mM L-glutamine (Sigma-Aldrich) in a 5% CO_2 incubator, as described previously (13). For hypoxic exposure, the culture medium was changed to a glucose-deprivation buffer and cells were transferred to an anaerobic chamber with an atmosphere of 5% CO_2 and 95% N_2 at 37°C for 5 h, as described elsewhere (13). Cells were then returned to standard culture medium for reoxygenation with 95% air, 5% CO_2 at 37°C for 20 h of recovery. Corresponding control cells were incubated at 37°C with 95% air, 5% CO_2 for the same time. When required, SH-SY5Y cells were pretreated with KHG26702 for 30 min, prior to OGD–R.

Determination of cell viability

Cell viability was assessed by 3-(4,5-dimethylthiazol-2-yl)-2,5-diphenyltetrazolium bromide (MTT) assay as described previously (1). The dark blue formazan crystals that formed in intact cells were solubilized with MTT lysis buffer, and optical density at 570 nm was measured with an ELISA microplate reader (Molecular Devices, Sunnyvale, CA, USA). The results were expressed as the percentage of the values for control cells. Cell death was also quantified by measuring LDH activity released into the medium, with an LDH assay kit (Roche, Mannheim, Germany), according to the manufacturer's instructions. The results were expressed as the percentage of LDH released from OGD–R-treated cells.

Measurement of ROS production, SOD activity, and levels of MDA, PGE_2, IL-6, and GSH

To monitor the accumulation of ROS, a microfluorescence assay with 2',7'-

dichlorodihydrofluorescein diacetate was used. The intensity of fluorescent dichlorofluorescein product was determined with a SpectraMax GEMINI XS fluorescence spectrophotometer (Molecular Devices) at an excitation wavelength of 485 nm and an emission wavelength of 538 nm. All experiments were performed in the dark. MDA levels were determined by lipid peroxidation assay kit, according to the manufacturer's instructions (Cayman, Ann Arbor, MI, USA). IL-6 and PGE_2 levels were measured with ELISA kits following the manufacturer's protocols (R&D Systems, Minneapolis, MN, USA); the results were determined with a microplate reader (Molecular Devices).

SOD activity was measured using a SOD assay kit (Cayman) by monitoring the formation of red formazan from the reaction of 2-(4-iodophenyl)-3-(4-nitrophenol)-5-phenyltetrazolium chloride and superoxide radicals by absorbance at 505 nm. One unit of SOD activity was defined as the amount of SOD required for 50% inhibition of red formazan formation.

Reduced GSH concentrations were measured in protein-free extracts as described elsewhere, with minor modifications (13). Briefly, 100 μL of 6 mM 5′,5′-dithio-bis(2-nitrobenzoic acid), 25 μL of protein-free extract, 875 μL of 0.3 mM NADPH, and 10 μL of GSH reductase (10 U/mL) were mixed to assay GSH contents. Absorbance changes were monitored at 412 nm spectrophotometrically. Intracellular GSH contents were calculated by reference to a standard curve generated with known amounts of GSH.

Western blotting

Proteins in crude extracts were separated by 10% sodium dodecyl sulfate–polyacrylamide-gel electrophoresis. Resolved proteins were transferred onto nitrocellulose membranes and blotted with primary antibodies to caspase-3, Bcl-2, and becn-1. Reactive protein bands were detected with an enhanced chemiluminescence detection kit according to the manufacturer's

instructions (Amersham, Buckinghamshire, UK). β-Actin was assessed for confirmation of equal protein loading for all samples. Densitometry was performed using Image J software (NIH, Bethesda, MD, USA).

Measurement of Aβ levels and secretase activity

$A\beta_{40}$ and $A\beta_{42}$ levels were detected with commercial ELISA kits (Invitrogen, Carlsbad, CA, USA), according to the manufacturer's instructions. Activities of β-secretase and γ-secretase were measured with a β-secretase activity fluorometric assay kit (Sigma-Aldrich) and a γ-secretase activity assay kit (R&D Systems), respectively, following the manufacturers' protocols.

Statistical analysis

Results are expressed as means ± SD of three independent experiments. Statistical significance for differences between groups was evaluated by one-way analysis of variance, followed by Student's *t*-test, and values of $p < 0.01$ were considered significant.

Conflicts of interest

The authors declare no conflicts of interest.

Acknowledgments

This study was supported by a grant (2018-010) from the Asan Institute for Life Sciences, Asan Medical Center, Seoul, Korea.

References

1. Taveira M, Sousa C, Valentao P et al (2014) Neuroprotective effect of steroid alalkaloids on glutamate-induced toxicity by preserving mitochondrial membrane potential and reducing oxidative stress. J Steroid Biochem Mol Biol 140, 106-115
2. Nalivaevaa NN, Fisk L, Kochkina EG et al (2004) Effect of hypoxia/ischemia and hypoxic preconditioning/reperfusion on expression of some amyloid-degrading enzymes. Ann New York Aca Sci 1035, 21–33
3. Pluta R, Furmaga-Jabłońska W, Maciejewski R et al (2013) Brain ischemia activates β- and γ-secretase cleavage of amyloid precursor protein: significance in sporadic Alzheimer's disease. Mol Neurobiol 47, 425–434
4. Salminen A, Kauppinen A, Kaarniranta K (2017) Hypoxia/ischemia activate processing of Amyloid precursor protein: impact of vascular dysfunction in the pathogenesis of Alzheimer's disease. J Neurochem 140, 536–549
5. Shiota S, Takekawa H, Matsumoto SE et al (2013) Chronic intermittent hypoxia/reoxygenation facilitate amyloid-β generation in mice. J Alzheimers Dis 37, 325–333
6. Li L, Zhang X, Yang D et al (2009) Hypoxia increases Aβ generation by altering β- and γ-cleavage of APP. Neurobiol Aging 30, 1091–1098
7. Li Q, Wang HM, Wang ZQ et al (2010) Salidroside attenuates hypoxia-induced abnormal processing of amyloid precursor protein by decreasing BACE1 expression in SH-SY5Y cells. Neurosci Lett 481, 154–158
8. Margaill I, Plotkine M, Lerouet D (2005) Antioxidant strategies in the treatment of stroke. Free Radic Biol Med 39, 429–443
9. Gould E (2007) How widespread is adult neurogenesis in mammals? Nat Rev Neurosci 8, 481–488
10. Carboni S, Hiver A, Szyndralewiez C et al (2004) AS601245 (1,3-benzothiazol-2-yl (2-[[2-(3-pyridinyl) ethyl] amino]-4 pyrimidinyl) acetonitrile): a c-Jun NH2-terminal protein kinase inhibitor with neuroprotective properties. J Pharmacol Exp Ther 310, 25–32
11. Choi MM, Kim EA, Hahn HG et al (2007) Protective effect of benzothiazole derivative KHG21834 on amyloid beta-induced neurotoxicity in PC12 cells and cortical and mesencephalic neurons. Toxicology 239, 156–166

12. Miglio G, Varsaldi F, Francioli E, et al (2004) Cabergoline protects SH-SY5Y neuronal cells in an in vitro model of ischemia. Eur J Pharmacol 489, 157–165
13. Fallarini S, Miglio G, Paoletti T, et al (2009) Clovamide and rosmarinic acid induce neuroprotective effects in in vitro models of neuronal death. Br J Pharmacol 157, 1072–1084
14. Lewen A, Matz P, Chan PH (2000) Free radical pathways in CNS injury. J Neurotrauma 17, 871–890
15. Urabe T, Yamasaki Y, Hattori N et al (2000) Accumulation of 4-hydroxynonenal-modified proteins in hippocampal CA1 pyramidal neurons precedes delayed neuronal damage in the gerbil brain. Neuroscience 100, 241–250
16. Kunwar A, Sandur SK, Krishna M et al (2009) Curcumin mediates time and concentration dependent regulation of redox homeostasis leading to cytotoxicity in macrophage cells. Eur J Pharmacol 611, 8–16
17. Katoh S, Mitsui Y, Kitani K et al (1999) Hyperoxia induces the neuronal differentiated phenotype of PC12 cells via a sustained activity of mitogen-activated protein kinase induced by Bcl-2. Biochem J 338, 465–470
18. Conrad M, Sato H (2012) The oxidative stress-inducible cystine/glutamate antiporter, system x (c) (-):cystine supplier and beyond. Amino Acids 42:231–246
19. Le DA, Wu Y, Huang Z et al (2002) Caspase activation and neuroprotection in caspase-3-deficient mice after in vivo cerebral ischemia and in vitro oxygen glucose deprivation. PNAS 99, 15188–15193
20. Niwa M, Hara A, Iwai T, et al (2001) Caspase activation as an apoptotic evidence in the gerbil hippocampal CA1 pyramidal cells following transient forebrain ischemia. Neurosci Lett 300, 103–106
21. Wang, Q, Sun AY, Simonyi A et al (2005) Neuroprotective mechanisms of curcumin against cerebral ischemia-induced neuronal apoptosis and behavioral deficits. J Neurosci Res 82, 138–148
22. Zhao H, Yenari MA, Cheng D et al (2003) Bcl-2 overexpression protects against neuron loss within the ischemic margin following experimental stroke and inhibits cytochrome c translocation and caspase-3 activity. J Neurochem 85, 1026–1036
23. Karch J, Molkentin JD (2015) Regulated necrotic cell death: the passive aggressive side of Bax and Bak. Circ Res 116, 1800–1809
24. Braak H, Braak E, Bohl J (1993) Staging of Alzheimer-related cortical destruction. Eur

Neurol 33, 403– 408

25. Suzuki WA, Amaral DG (2004) Functional neuroanatomy of the medial temporal lobe memory system. Cortex 40, 220–222
26. Banati RB, Gehrmann J, Wiessner C et al (1995) Glial expression of the beta-amyloid precursor protein (APP) in global ischemia. J Cereb Blood Flow Metab 15, 647–654
27. Webster NJ, Green KN, Peers C et al (2002) Altered processing of amyloid precursor protein in the human neuroblastoma SH-SY5Y by chronic hypoxia. J Neurochem 83, 1262–1271
28. Mattson MP (2004) Pathways towards and away from Alzheimer's disease. Nature 430, 631–639
29. Müller UC, Deller T, Korte M (2017) Not just amyloid: physiological functions of the amyloid precursor protein family. Nat Rev Neurosci 18, 281–298
30. Yu WH, Cuervo AM, Kumar, A et al (2005) Macroautophagy-a novel Beta-amyloid peptide generating pathway activated in Alzheimer's disease. J Cell Biol 171, 87–98

Figure legends

Fig. 1. Effects of oxygen–glucose deprivation–reoxygenation (OGD–R) and KHG26702 on cell viability in SH-SY5Y cells. (A) Chemical structure of KHG26702. Cell viability was assessed by (B) the MTT reduction assay and (C) lactate dehydrogenase (LDH) assay. Data are presented as means ± SD, and are representative of three independent experiments. * indicates a significant difference between the OGD–R-treated group and the OGD–R group pretreated with KHG26702 ($p < 0.01$).

Fig. 2. Effects of KHG26702 on markers of oxidative stress, inflammation, and antioxidant activity. Levels of (A) reactive oxygen species (ROS) production, (B) malondialdehyde (MDA), (C) prostaglandin E_2 (PGE_2), (D) interleukin 6 (IL-6), (E) superoxide dismutase (SOD) activity, and (F) reduced glutathione (GSH) in oxygen–glucose deprivation–reoxygenation (OGD–R)-treated SH-SY5Y cells and controls, with and without pretreatment with KHG26702. Data are presented as means ± SD and are representative of three independent experiments. * indicates a significant difference between the OGD–R group and the OGD–R group pretreated with KHG26702 ($p < 0.01$).

Fig. 3. Effects of oxygen–glucose deprivation–reoxygenation (OGD–R) and KHG26702 on levels of caspase-3 and Bcl-2 apoptosis-related proteins in SH-SY5Y cells. (A) Equal amounts of crude cell extracts were separated by electrophoresis, transferred to nitrocellulose membranes, and immunoblotted with primary antibodies against the indicated proteins. (B, C) Bar graphs show the quantification of levels of caspase-3 and Bcl-2, calculated by densitometry. Data are presented as means ± SD, and are representative of three independent experiments. * indicates a significant difference between the OGD–R-treated group and the

OGD–R group pretreated with KHG26702 ($p < 0.01$).

Fig. 4. Effects of oxygen–glucose deprivation–reoxygenation (OGD–R) and KHG26702 on β-amyloid (Aβ) levels, secretase activity, and becn-1 levels in SH-SY5Y cells. Levels of (A) $A\beta_{40}$ and (B) $A\beta_{42}$ were determined by ELISA. Activities of (C) β-secretase and (D) γ-secretase were determined with activity assay kits as described in Materials and Methods. (E) Western blotting and (F) densitometric analysis were performed as described in Fig. 3. Data are presented as means ± SD and are representative of three independent experiments. * indicates a significant difference between the OGD–R-treated group and the OGD–R group pretreated with KHG26702 ($p < 0.01$).

(A)

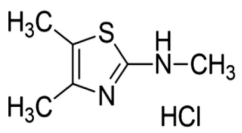

Chemical Structure of KHG26702

(B)

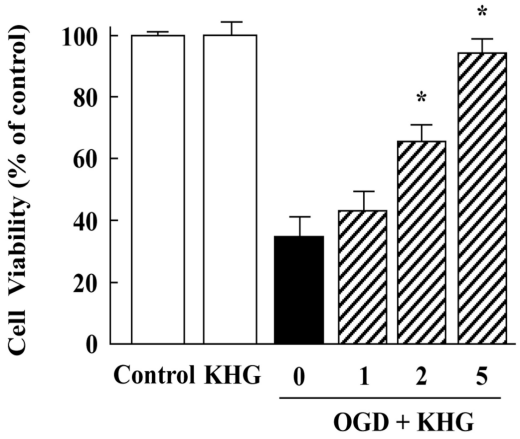

(C)

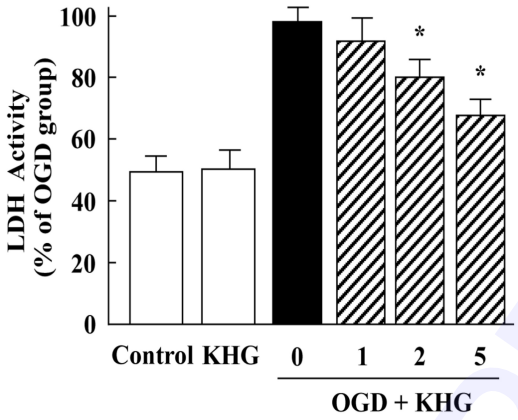

Fig. 1.

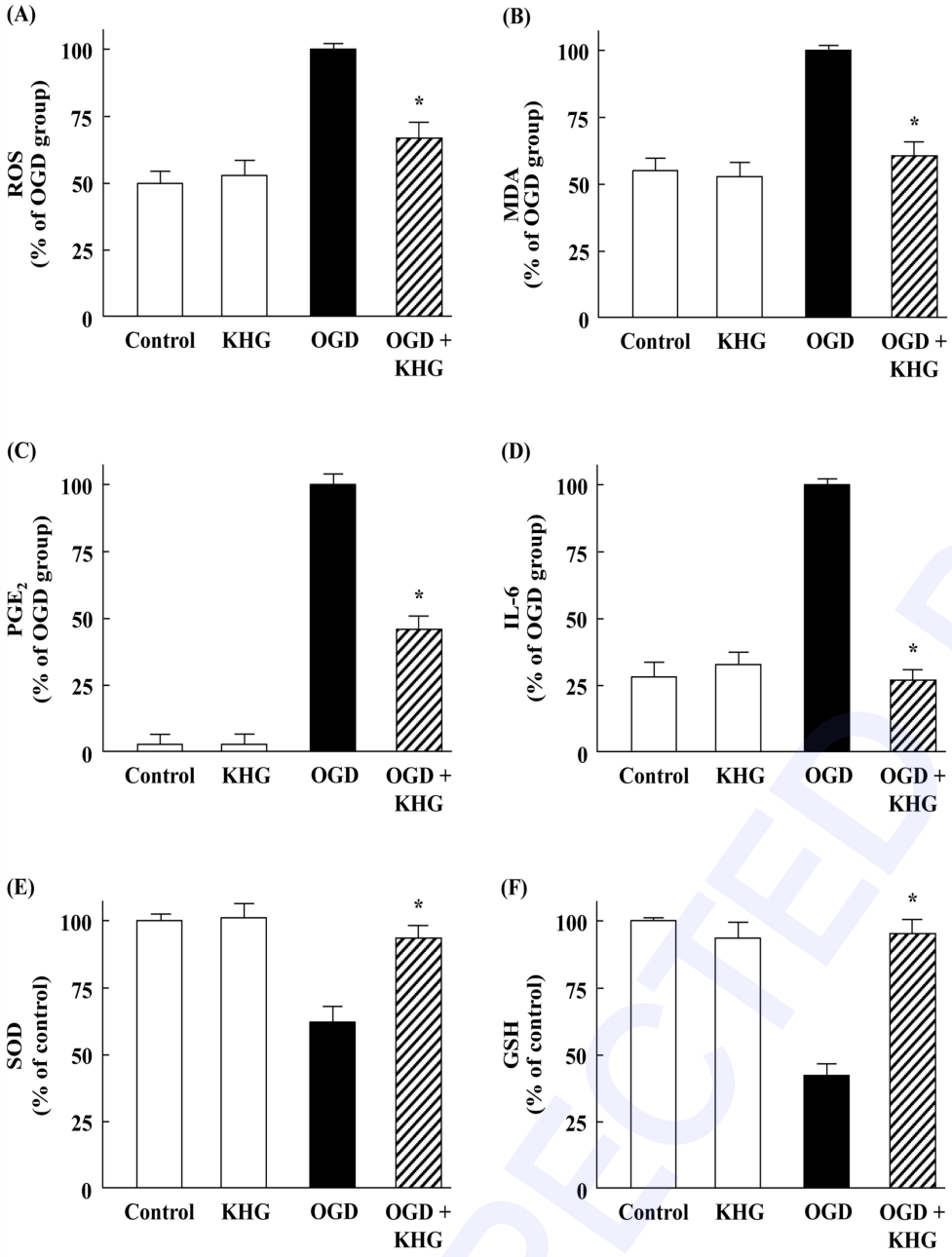

Fig. 2.

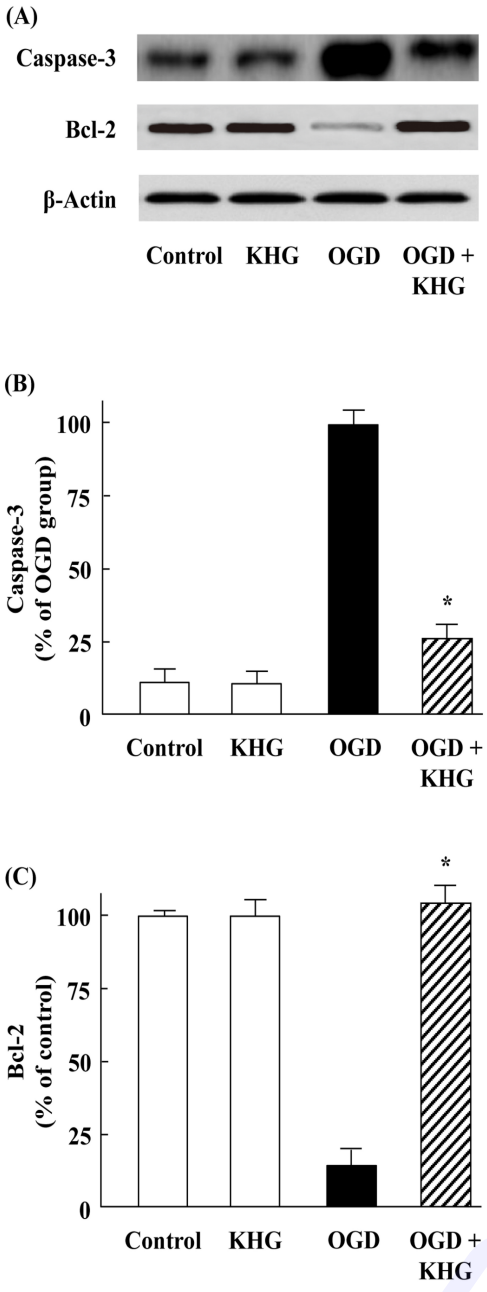

Fig. 3.

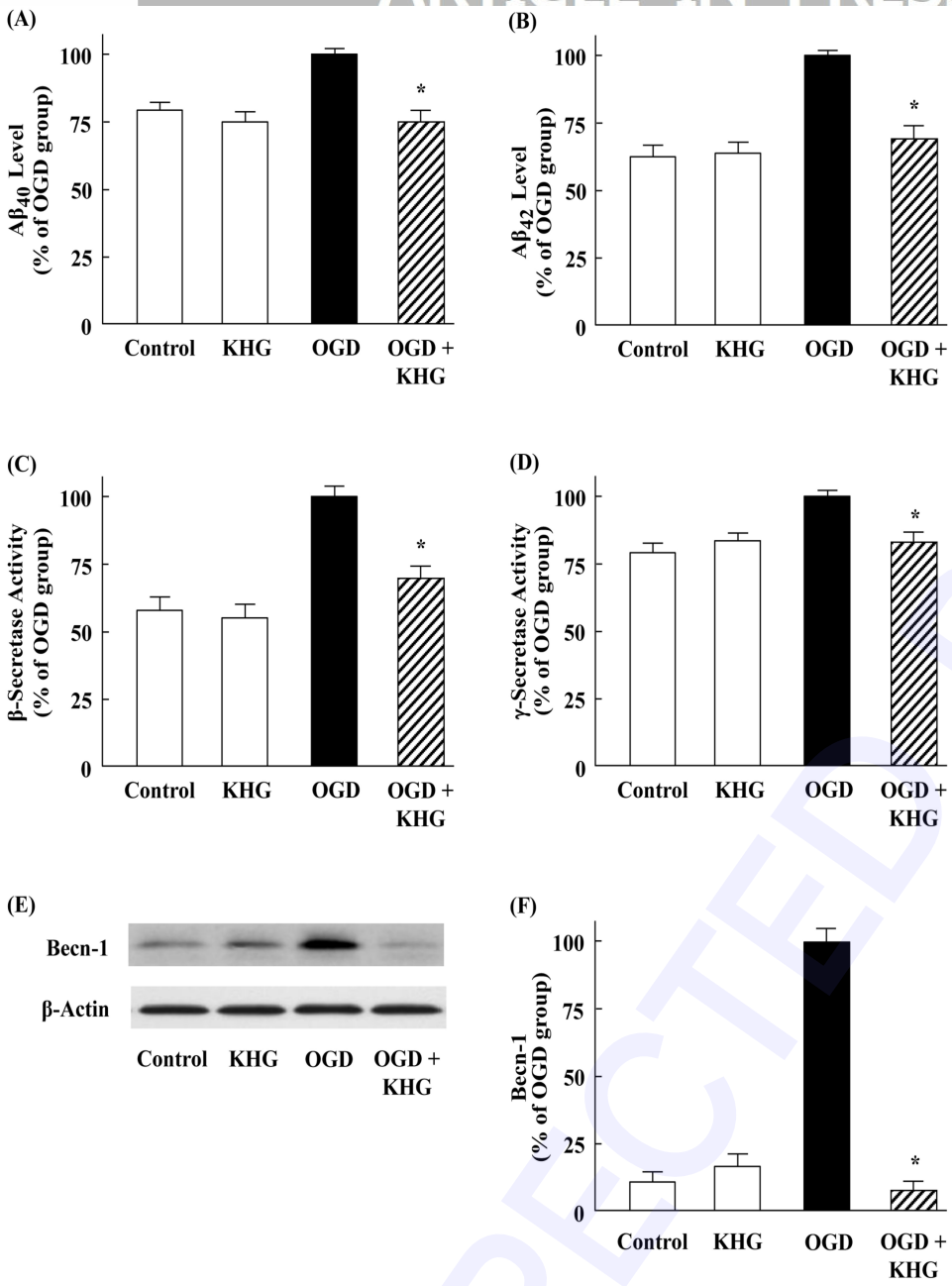

Fig. 4.